MEMBRANE FUSION DURING SECRETION

A Hypothesis Based on Electron Microscope Observation of *Phytophthora Palmivora* Zoospores during Encystment

PEDRO PINTO da SILVA and MARIA LUIZA NOGUEIRA

From the Laboratory of Pathophysiology, National Cancer Institute, National Institutes of Health, Bethesda, Maryland 20014 and the Department of Plant Pathology, University of California Riverside, Riverside, California 92502

ABSTRACT

Interpretation of freeze-fracture and thin-section results shows that fusion of the peripheral vesicle with the plasmalemma of a *Phytophthora palmivora* zoospore occurs at several discrete sites and results in the formation and expansion of a particle-free bilayer membrane diaphragm and in the appearance of a polymorphic network of membrane-bounded tunnels, the lumina of which are continuous with the cytoplasm. The outer half of the bilayer membrane diaphragm appears continuous with the outer half of the plasma membrane; the inner half of the bilayer membrane diaphragm with the inner half of the peripheral vesicle membrane; and the inner half of the plasmalemma with the outer half of the peripheral vesicle membrane.

Interpretation of our results leads us to formulate a hypothesis for a sequence of several intermediate stages involved in membrane fusion. The initial fusion event is viewed as a local catastrophe (Thom, R. 1972. Stabilité Structurelle et Morphogenèse. W. A. Benjamin Inc., Reading, Mass.) involving the sudden reorganization of apposed elements of the inner half of the plasmalemma and the outer half of the peripheral vesicle membrane. Fusion of apposed components at the rim of the perimeter of fusion results in the formation of a toroid hemi-micelle which provides continuity between the inner half of the plasmalemma and the outer half of the peripheral vesicle membrane. Simultaneously, apposed components at the site of fusion may reorganize into an inverted membrane micelle. A bilayer membrane diaphragm is then formed by apposition and flowing of components form the outer half of the plasmalemma and the inner (exoplasmic) half of the peripheral vesicle membrane. The existence of large areas of membrane contact before fusion may lead to several fusion events and the formation of a polymorphic network of membrane-bound tunnels.

Membrane fusion is a frequent and important event in the life of most eukaryotic cells (17, 23, 29, 30). Among other cellular processes, membrane fusion mediates secretion as a necessary step to the transfer of macromolecules contained within cytoplasmic vesicles to the cell periphery or

the extracellular space (23).

The sequence of events during membrane fusion has been divided into four stages (29): (*a*) close approximation and contact; (*b*) induction, i.e., the establishment of an adequate physical-chemical milieu at (or near) the site of fusion; (*c*) fusion proper, i.e., the establishment of intermembrane linkages; and (*d*) stabilization, i.e., the reestablishment of a physical-chemical equilibrium within the region of fusion. The third stage of fusion must involve considerable rearrangement of membrane components within a restricted domain. Palade and Bruns (24) analyzed high resolution profiles of plasmalemmal vesicles of vascular endothelia and proposed that, after close apposition of the membranes (observed as a pentalaminar profile), membrane reorganization led to progressive elimination of layers and resulted in the appearance of one membrane (observed as a trilaminar profile) common to both the plasma membrane and the membrane of the fusing vesicle. Continuity of spaces (vesicle lumen and extracellular space) occurred either by destabilization of this common membrane (by destruction and/or reabsorption) or by its further reorganization into a single-layered diaphragm (i.e., not containing a bilayer membrane).

The introduction of freeze-fracture and freeze-etch techniques made it possible to overcome inherent limitations of thin-section techniques because they provided images that contained information relative to the planar distribution of membrane components instead of averaged electron density profiles of stainable components in cross-sectioned membranes. Using these techniques, Satir and co-workers (33, 34) observed membrane fusion during mucocyst secretion in *Tetrahymena* and proposed a model for membrane reorganization during fusion which is qualitatively different from that of Palade and Bruns. Briefly, a rosette of membrane particles (thought to represent protein-containing intramembrane structures) was formed before fusion. Membrane apposition, fusion, and stabilization did not involve the formation of a bilayer membrane diaphragm but, instead, the brief formation of a system of micelles and separated membrane halves leading to incorporation of the vesicle membrane into the plasmalemma and release of secretory product.

The process of encystment in *Phytophthora palmivora* zoospores (Fig. 1) involves the fusion of peripheral vesicles (13, 14) with the plasmalemma followed by the release of glycoprotein and, possibly, other cell wall precursor materials (14, 35, footnote 1). This is a secretory process (14, 23) adequate to the study of membrane morphology because it is possible, by stirring zoospore suspensions, to accelerate encystment: the zoospore, a natural protoplast (3), becomes a cyst with a complete cell wall within 2 min (39). In this report, we have analyzed the freeze-fracture and thin-section morphology of the fusion of peripheral vesicles with the plasma membranes of *P. palmivora* zoospores during the initial stages of encystment. Our results support and extend the observations of Palade and Bruns (24) and of Palade (23), and demonstrate that the formation of a particle-free bilayer membrane diaphragm is a step which follows the initial fusion events but which precedes release of the vesicle contents to the extracellular space. Analysis of our micrographs and of those available in other ultrastructural studies of membrane fusion leads us to propose a hypothesis of the sequence of reorganization of membrane components during membrane fusion.

MATERIALS AND METHODS

P. palmivora (strain P113, isolated from papaya; earlier designated *P. parasitica*) was grown at 25°C on V-8 juice agar plates for 3–4 days in the dark followed by 3–4 days of illumination under fluorescent lights (2, 39). Sporulated cultures were chilled at 1°C for 10 min and the plates flooded with 15 ml of distilled water. Numerous zoospores were liberated and the suspension was filtered through Whatman #41 filter paper (Whatman Inc., Clifton, N.J.) to remove fragments of mycelium or sporangia. Encystment was accelerated by vigorous stirring with a Vortex mixer (39). Samples were stirred for 0, 45, and 75 s. Zoospores were fixed in 1% glutaraldehyde in 0.1 M potassium phosphate buffer, pH 7.2. The samples were fixed at room temperature for 30 min, washed with buffer, resuspended in buffer, and stored in the refrigerator. After fixation, part of the zoospores was resuspended in about 1 ml of buffer. 14 ml of a 25% glycerol solution in phosphate buffer was added dropwise at room temperature over a period of 10 min to the resuspended zoospores. The suspension was centrifuged at 1,000 *g* for 10 min, the supernate was removed, and fresh 25% glycerol solution was added. The material was then incubated for 30 min at 37°C and for 1 h at room temperature. The material was frozen in the liquid phase of partially solidified Freon 22, freeze-fractured at −110°C in a Balzers 510 unit (Balzers High Vacuum Corp., Santa Ana, Calif.), and immediately shadowed with a platinum-carbon electron gun. The micrographs

[1] Nogueira, M. L., P. Pinto da Silva, and S. Bartnicki-Garcia. Submitted for publication.

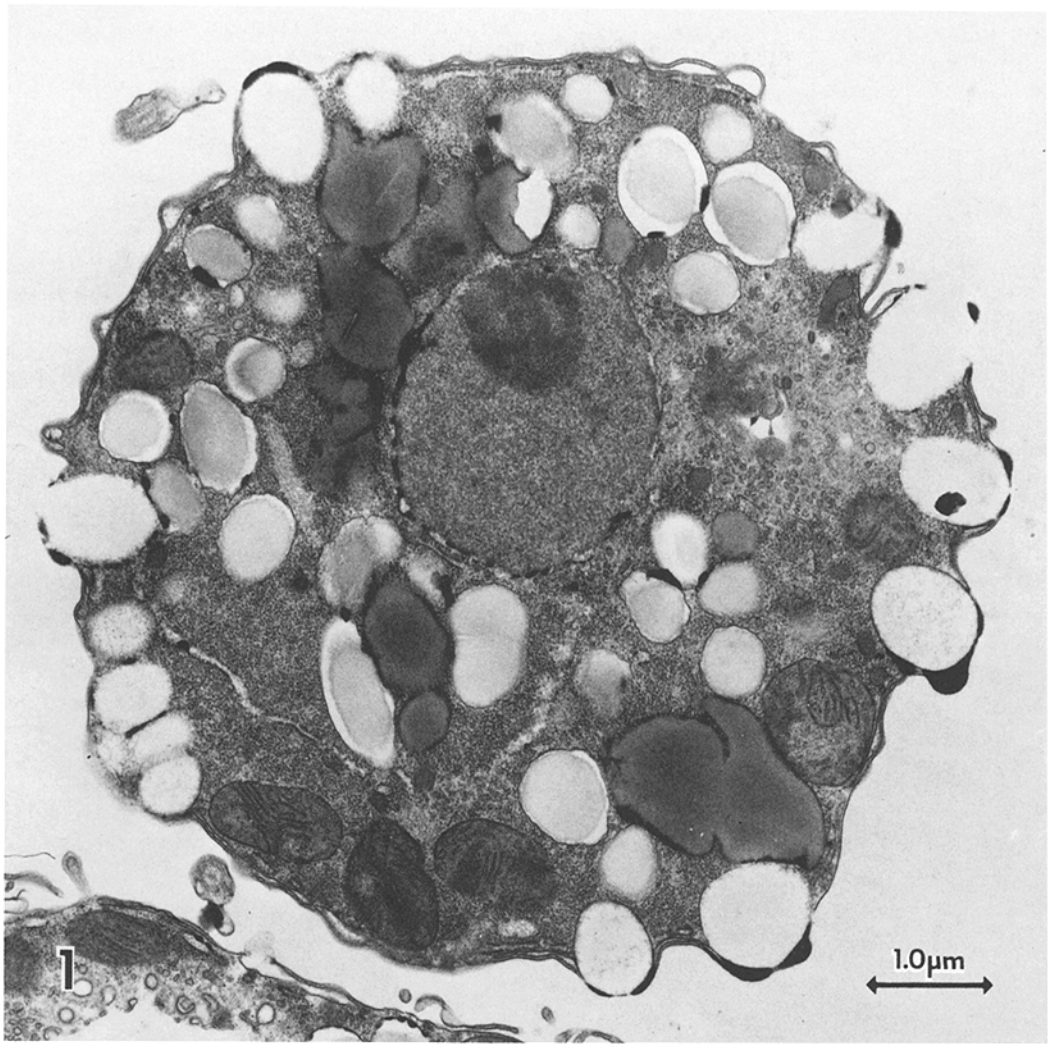

FIGURE 1 *Phytophthora palmivora* zoospore. Peripheral vesicles are seen adjacent to the plasmalemma. A layer of "flat vesicles" (4, 15) is also seen in close proximity to the plasmalemma. × 16,500.

were mounted with the metal shadowing direction from bottom to top. Shadows are white.

Thin-section observations were also made in order to confirm the membrane nature of the bilayer membrane diaphragm as indicated by interpretation of freeze-fracture results. For thin section, zoospores were fixed in 2% glutaraldehyde in 0.1 M Na-cacodylate buffer, pH 7.2, for 2 h at room temperature, post-fixed in 1% OsO_4 in the same buffer for 1 h, dehydrated, embedded in Epon, and sectioned with a diamond knife.

RESULTS

Freeze-fracture

Freeze-fracture splits biological membranes (5, 25). Consequently, (*a*) the particle-free regions of face A originate from membrane domains with bilayer organization and provide views of the outer face of the inner half of these membrane regions; (*b*) the particles seen on face A represent intercalated sites where the bilayer organization is interrupted and provide views of protrusions originally embedded in the outer membrane half; and (*c*) the smooth regions of face B represent the inner face of the outer membrane half interrupted by a smaller number of particles that represent protrusions originally embedded in the inner half of the membrane. The nomenclature of fracture faces follows the diagram in Fig. 16*b* which sum-

marizes the interpretation of the results as given in sections (*a*) and (*b*) of the first part of the Discussion section.[2] Although much of the figure legend text describes the results, their meaning is more completely understood accompanying the discussion.

Observation of the fracture faces of plasma membranes fixed after 0–45 s of stirring frequently showed circumscribed areas where the fracture plane of the plasma membrane was substituted by a polymorphic network of fracture faces (Figs. 2, 4–11). In these areas, fracture face A of the plasmalemma (pm_A) and a convex network (ut_A) delimited smooth areas ($d_B{}^v$) where particles were rarely observed (Figs. 2, 6, and 7). In other instances, the network was seen as concave particle-poor regions (lt_B; Figs. 7 and 8). Convex (ut_A) and concave (lt_B) elements frequently coexisted on the same circumscribed network (Fig. 7). In all cases, convex regions of the network (ut_A) were elevated relative to the smooth regions ($d_B{}^v$) (Figs. 2, 6, and 7), whereas the concave regions of the network (lt_B) were at a lower level relative to the smooth regions (Figs. 7 and 8). The convex regions of the membrane network could be seen to be continuous with fracture face A of the plasma membrane (Figs. 2, 6, and 7). Conversely, fracture face A of the plasma membrane could be seen to be contiguous but not continuous with the concave, particle-poor areas of the network (Fig. 8, curved white arrows).

Examination of regions of close membrane apposition as seen from the cell interior revealed aspects complementary to those described above (Figs. 9–11). It was possible to ascribe these aspects to regions where peripheral vesicles (v_A) were in close contact with the plasma membrane (Fig. 9). Fracture face B of the plasma membrane (pm_B) was interrupted by a complex system consisting of a network of particle-containing fracture faces (lt_A and ut_B) interspersed with smooth regions ($d_B{}^{pm}$) that were virtually free of particles (Figs. 9–11). Raised, convex areas of the network (lt_A) were particle-rich (Figs. 9–11), whereas concave areas of the membrane network (ut_B) were particle-poor (Figs. 9–11). In these fracture faces the concave aspects of the network (ut_B) could be seen to be continuous with fracture face B of the plasma membrane (Figs. 10 and 11). Occasionally, face B of the plasmalemma could be seen to be contiguous but not continuous with the convex, particle-rich network (Fig. 9, curved white arrow and Fig. 11, hollow white arrows). In these cases, the presence of convex regions of the network contiguous with concave areas of the plasmalemma indicated the presence of a lumen within the network, demonstrating its tunnel-like nature. In regions that demonstrated contiguous but not continuous aspects of the convex and concave network (i.e. cross fractures away from the rim of the fusion area), it could also be seen that both fracture faces represented different views of a single tunnel (Fig. 11, opposed arrowheads).

The smooth areas $d_B{}^v$ and $d_B{}^{pm}$ were frequently slightly convex (Fig. 2) or concave (Figs. 9 and 10). The smooth regions could be easily distinguished from fractured ice because of the granular appearance of the latter (Fig. 3,*i*). Occasionally, large rounded particles (Fig. 5 and Fig. 10, asterisk) or depressions (Fig. 8, arrowheads) could be observed on the otherwise smooth fracture faces. In some cells the smooth areas were very small (Fig. 4, hollow arrowheads) and coexisted with even smaller spot-like depressions (Fig. 4, solid white arrowheads).

Freeze-fracture of preparations of zoospores stirred for 75 s revealed also aspects after fusion, showing complete incorporation of the peripheral vesicle membrane into the plasmalemma (Fig. 3), which were not evident in unstirred preparations or in preparations stirred for 45 s. Freeze-fracture and freeze-etch aspects of vesicle discharge and cell wall formation are reported elsewhere (footnote 1).

[2] A recently proposed nomenclature of fracture faces (6) has not been used. We agree that the use of P (protoplasmic face) for the A face and E (exterior, exoplasmic face) for the B face provides a mnemonic which facilitates identification. However, the membrane particles observed on the P (or A) face correspond to portions of structures which, although probably intercalated across the entire apolar matrix of the membrane regions with bilayer organization, are embedded into the external (exoplasmic) half of the membrane. In the case of the erythrocyte ghost membrane, the particles represent intercalations which reach the external surface where they bear a variety of antigens, lectin-binding sites, anionic groups and influenza virus receptors (18). As a consequence, the term "protoplasmic" seems inadequate to define a membrane face in which the most significant features represent intercalations into the external half of the membrane. The use of a neutral nomenclature (A and B faces) lacking connotations seems, at present, preferable.

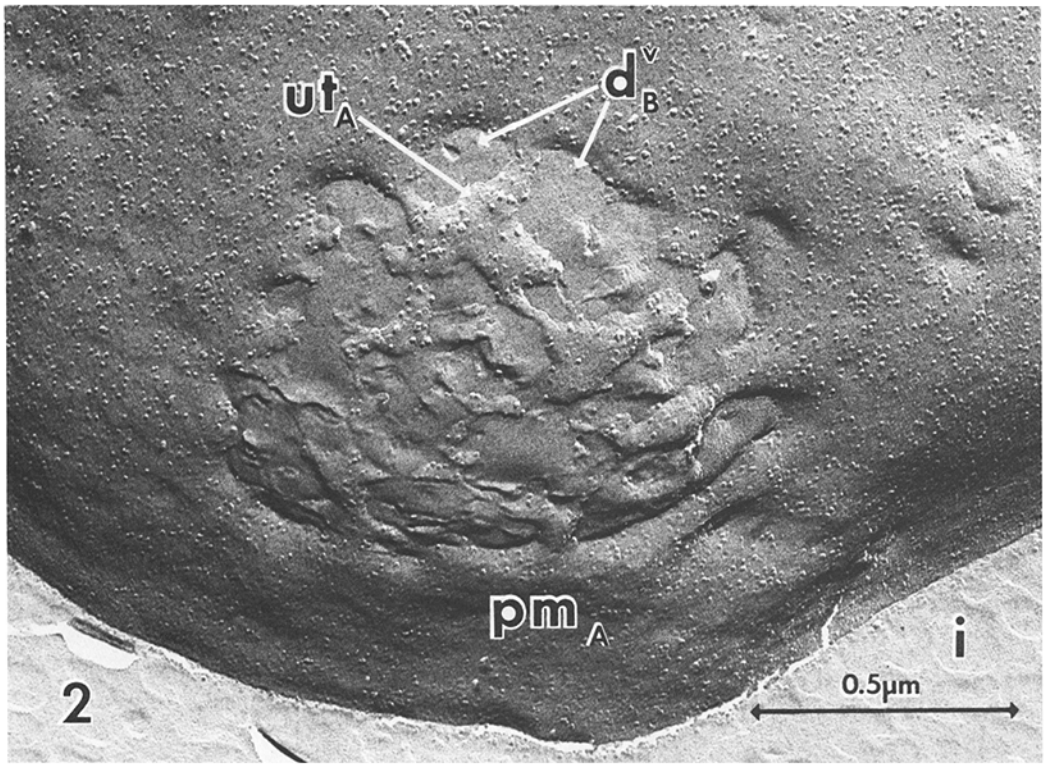

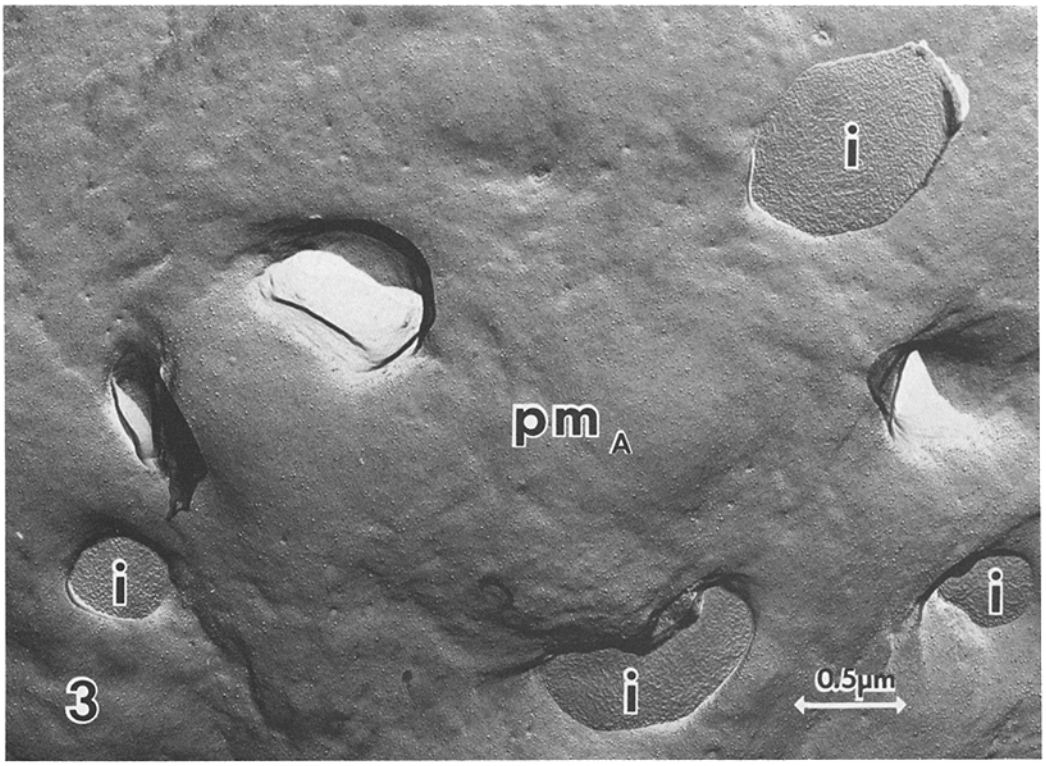

FIGURE 2 Fracture face A of *P. palmivora* zoospore. Network of particle containing membrane (ut_A) is continuous with the fracture face of the plasma membrane (pm_A) and delimits particle-free areas representing the fractured bilayer membrane diaphragm (d_B^v) (compare with Fig. 16*a*). × 70,000.

FIGURE 3 Fracture face A of *P. palmivora* zoospore (pm_A) illustrates completion of the process of fusion of peripheral vesicles and release of vesicular contents. Fracture through ice (*i*) shows granular eutectics which differentiate it from smooth faces produced by fracture of particle-free diaphragm (Fig. 2, d_B^v). × 30,000.

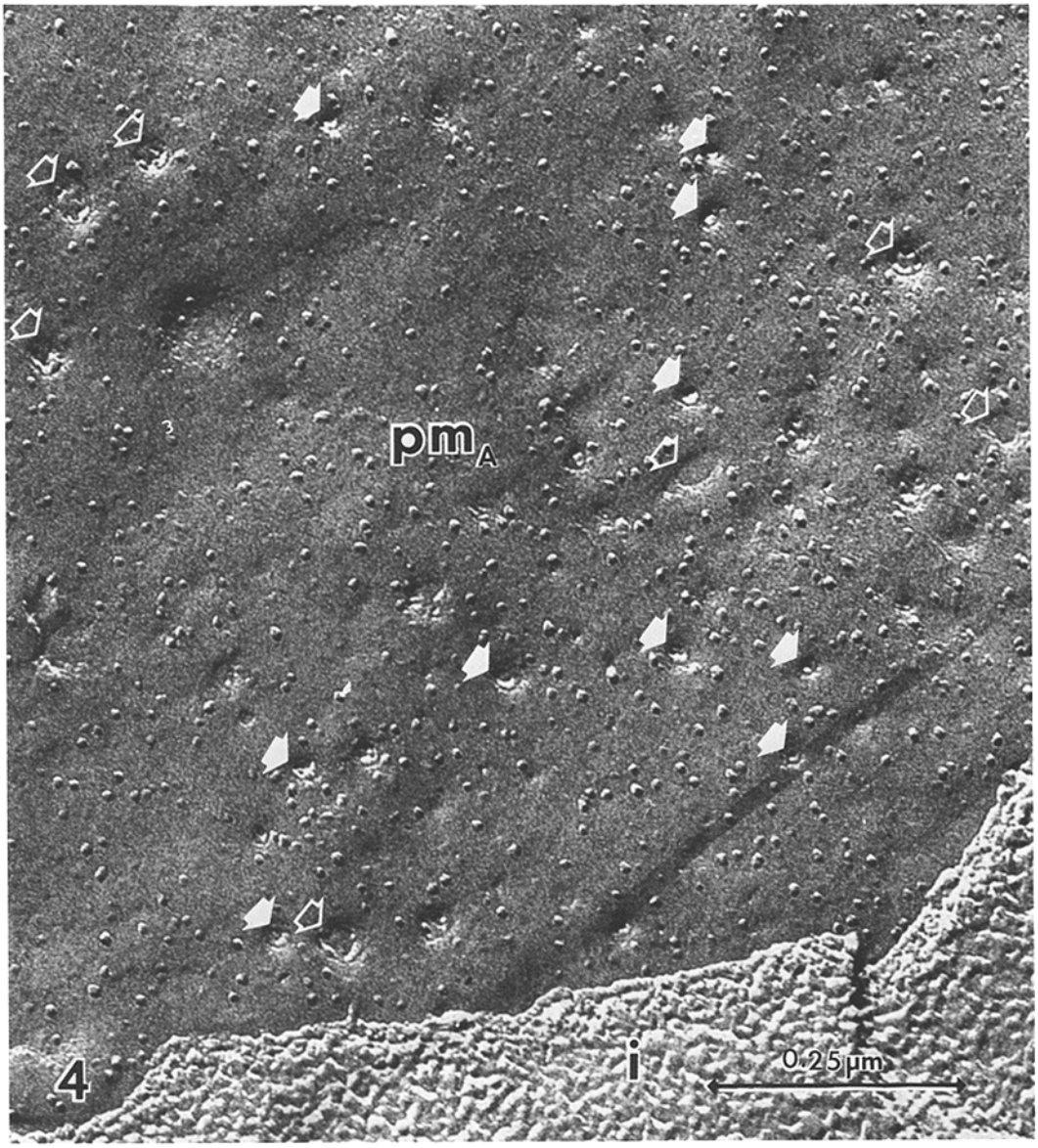

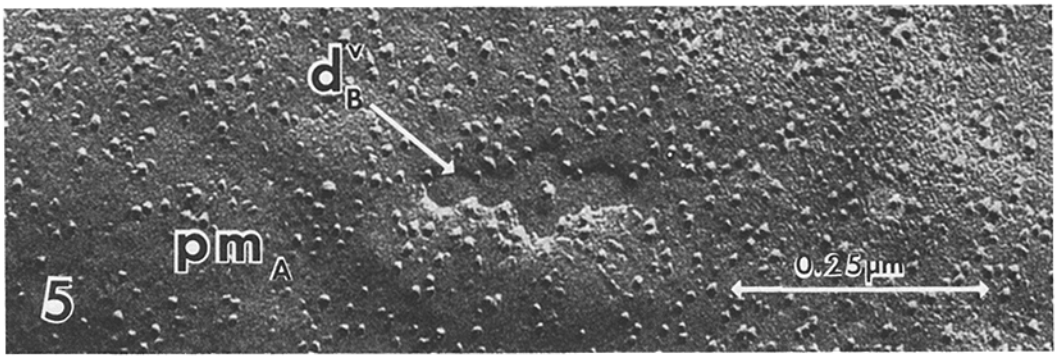

FIGURE 4 Fracture face A (pm_A) of the plasma membrane. Very small bilayer membrane diaphragms (hollow arrowheads) coexist with smaller areas which reveal a central rounded depression (solid arrowheads). Both aspects are thought to represent initial stages of fusion (see Discussion, II (*b*), 1 and Fig. 17 A). × 135,000.

FIGURE 5 Fracture face A (pm_A) and a bilayer membrane diaphragm ($d_B{}^v$). The diaphragm is thought of as expanding and to represent a stage following that shown in preceding micrograph. Note presence of single particle in center of otherwise particle-free diaphragm (see Discussion, II (*b*), 2 and Fig. 17 B and C). × 135,000.

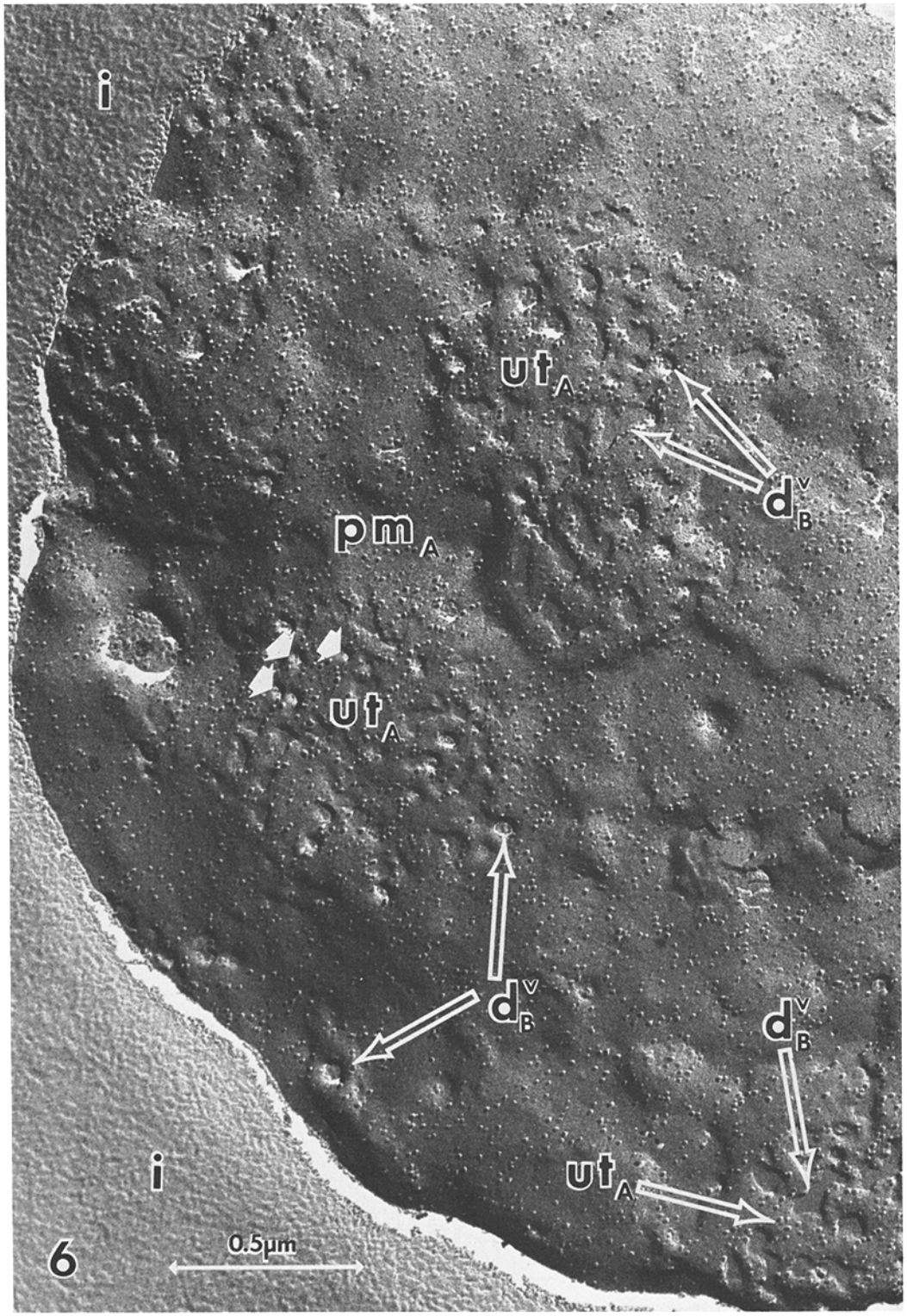

FIGURE 6 Fracture face A of plasmalemma (pm_A) is interrupted by several fields of bilayer membrane diaphragms (d_B^v) which delimit a particle-rich membrane network (ut_A) continuous with the plasma membrane. This micrograph is thought to reveal several stages of fusion, early (white arrowheads, center) to relatively advanced (lower right corner). × 60,000.

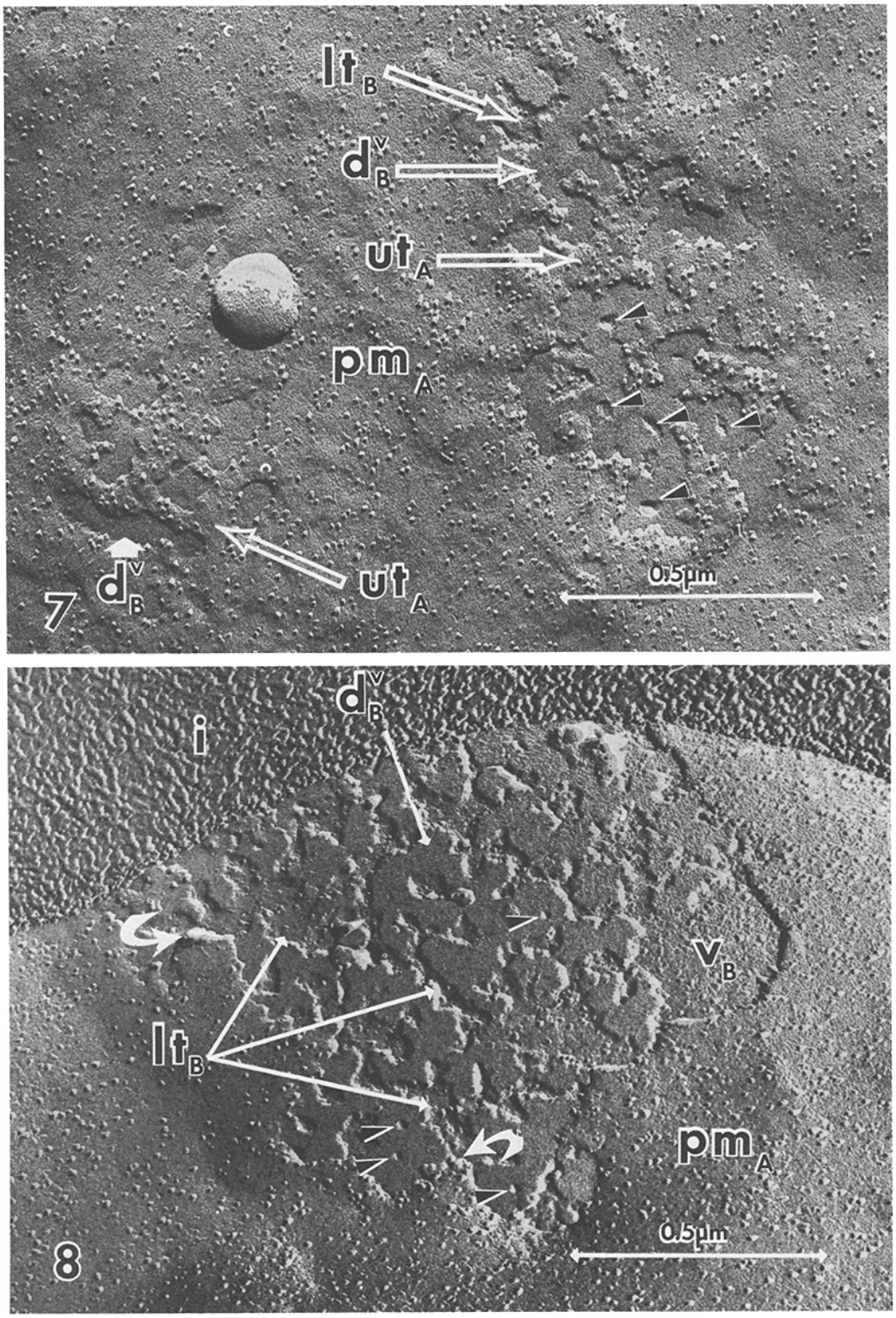

FIGURE 7 Fracture face A of zoospore plasma membrane (pm_A) shows smooth bilayer membrane diaphragm (d_B^v), particle-rich convex network (ut_A) and smaller portions of a particle-poor concave network (lt_B), including several areas which represent insular remnants of tubular network (black/white arrowheads). × 80,000.

FIGURE 8 Fracture face A of zoospore plasmalemma (pm_A) and bilayer membrane diaphragm (d_B^v) delimit concave, particle-poor network (lt_B). The network is continuous with the fracture face of the peripheral vesicle membrane (v_B) but discontinuous with the fracture face of the plasma membrane (white arrow). Four large, rounded depressions (black/white arrowheads) are seen on the diaphragm. × 80,000.

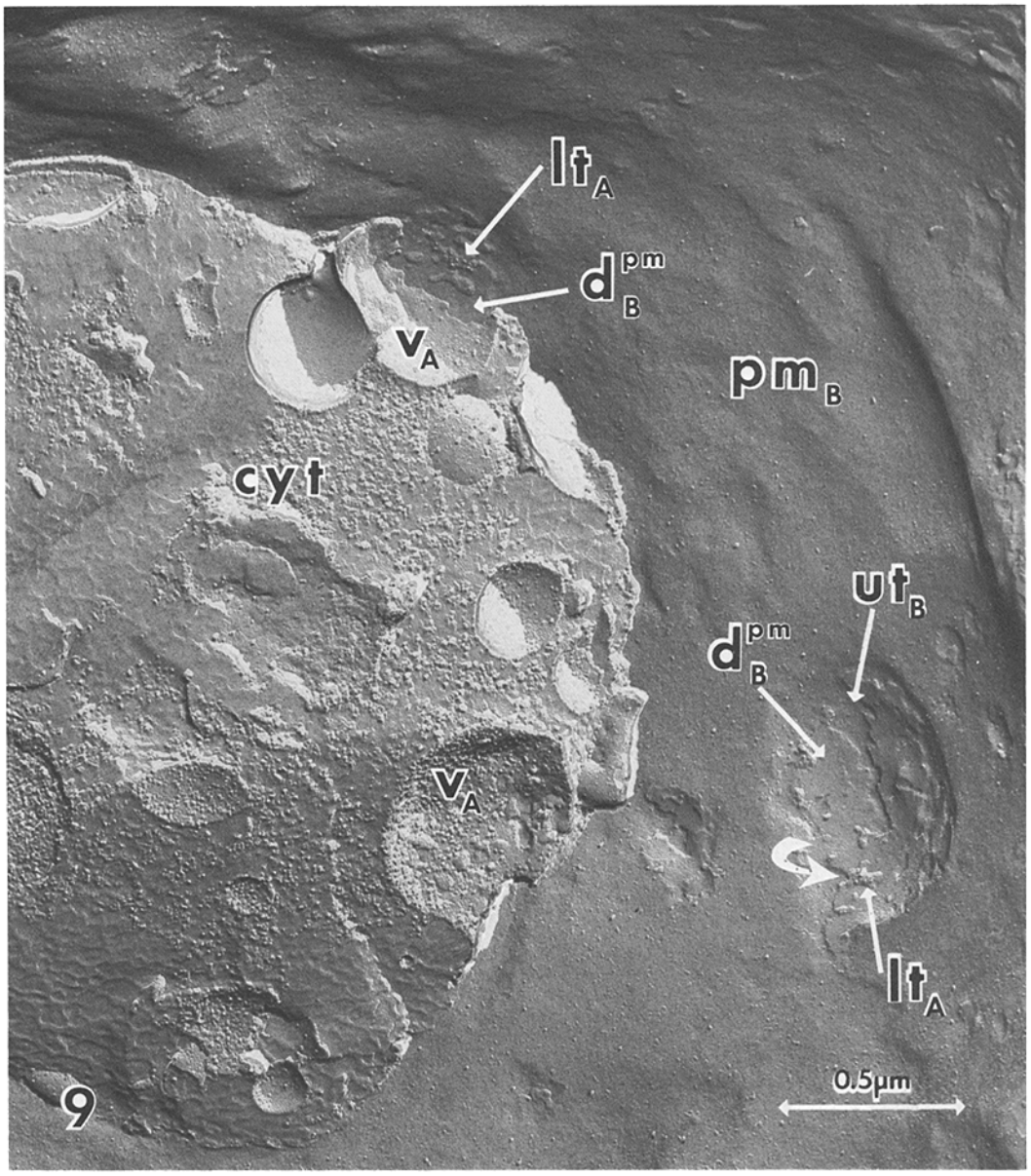

FIGURE 9 Peripheral vesicles (v_A) are seen inside the cell adjoining the plasmalemma (pm_B). Bilayer membrane diaphragm ($d_B{}^{pm}$) coexists with convex particle-rich (lt_A) or concave, particle-poor (ut_B) network. lt_A is contiguous but not continuous with pm_B and illustrates tunnel-like nature of network (white arrow). × 50,000.

Thin Section

Observation of thin sections of unstirred preparations of *P. palmivora* zoospores revealed the existence of membrane areas common to both the plasma membrane and the membrane of the peripheral vesicle (Figs. 12–14). The trilaminar profile of this membrane (here called bilayer membrane diaphragm) seemed continuous with both the trilaminar profile of the plasma membrane and that of the peripheral vesicle. This is illustrated in Fig. 14 (opposed arrowheads) where: (*a*) the outer dense line of the diaphragm appears continuous with the outer dense line of the plasma mem-

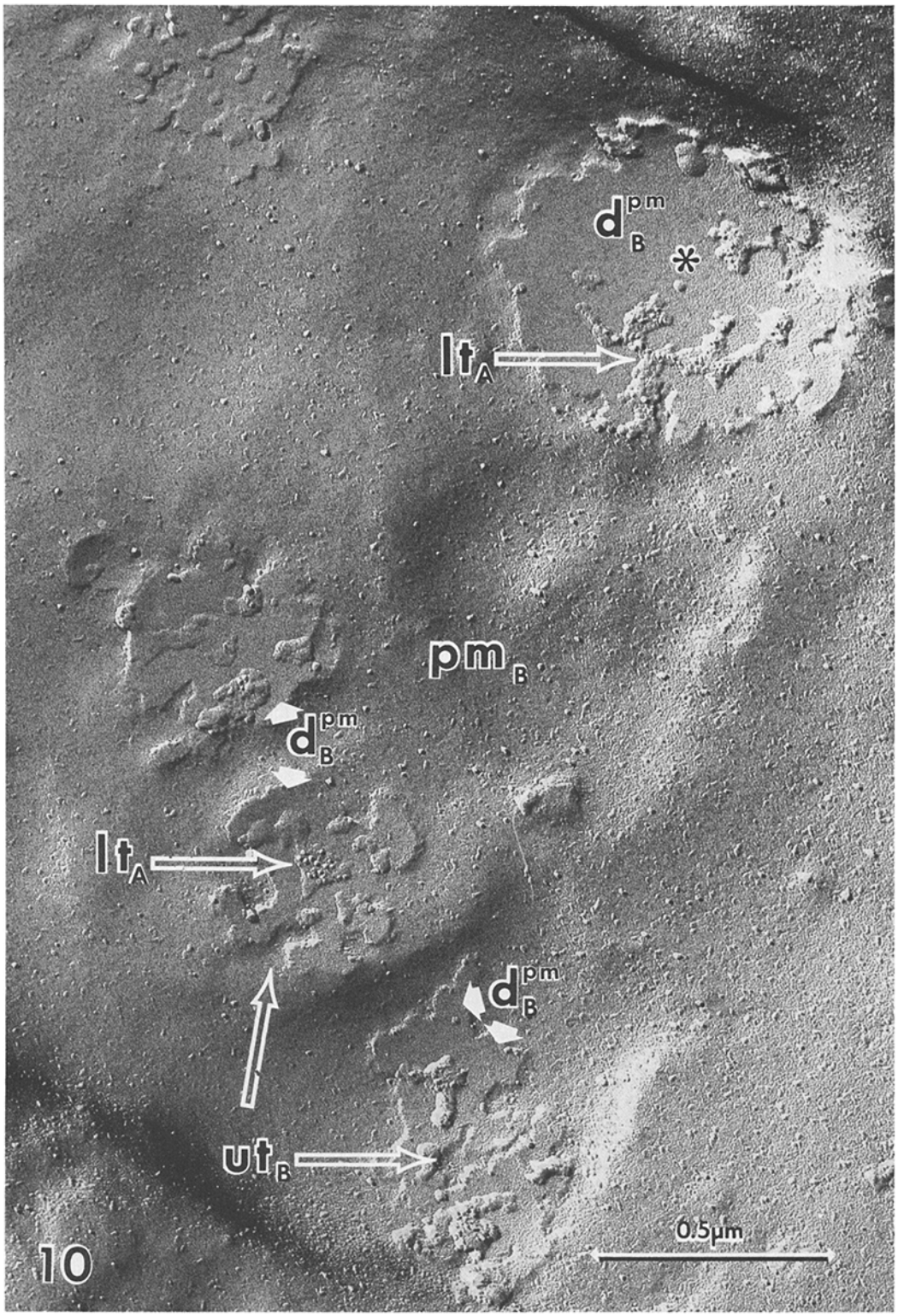

FIGURE 10 Fracture face of plasma membrane (pm_B) is interrupted by several smooth, slightly concave bilayer membrane diaphragms (d_B^{pm}), particle-rich convex network (lt_A) and particle-poor concave network (ut_B). Concave network is continuous with fractured plasma membrane. × 75,000.

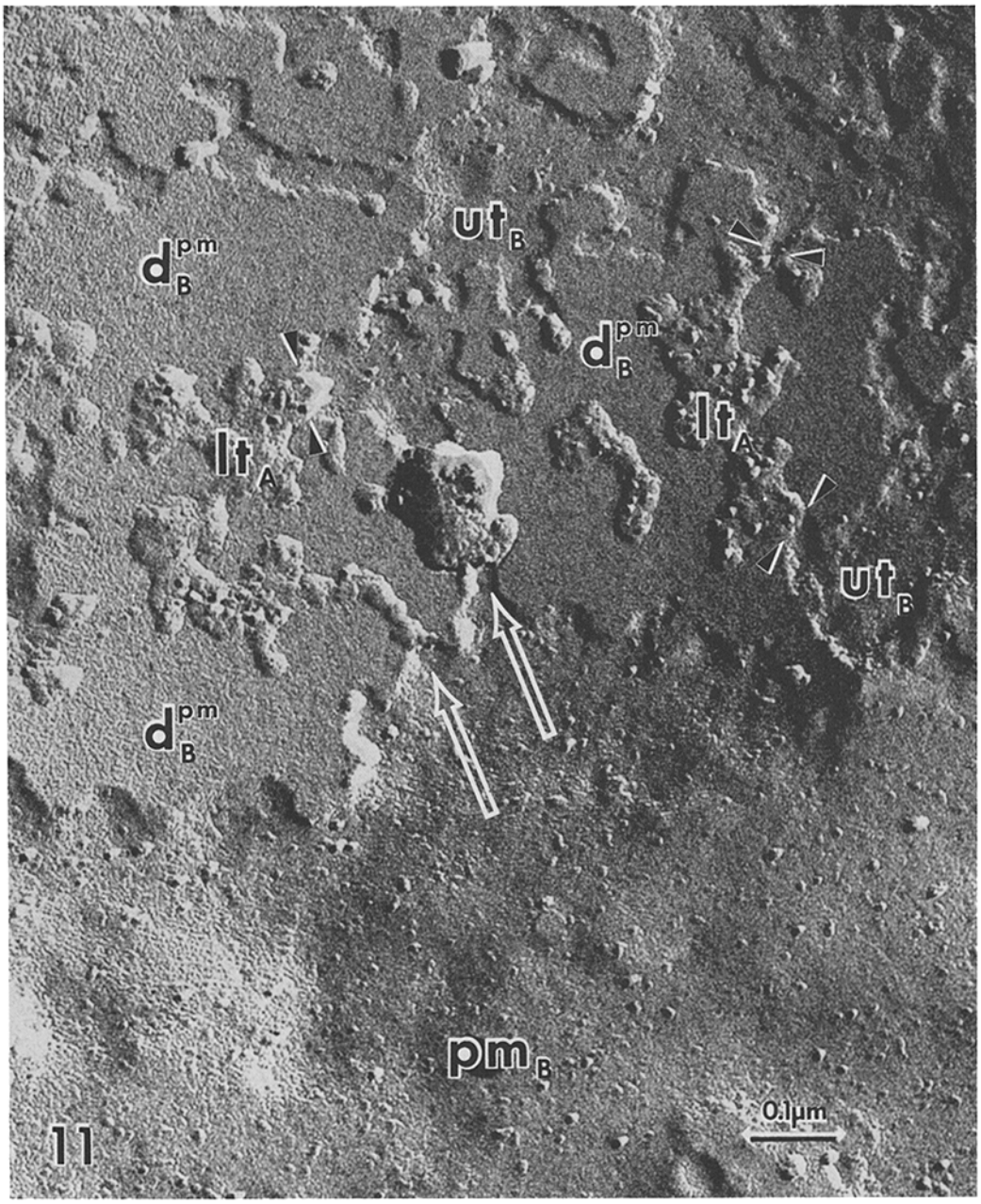

FIGURE 11 High magnification view reveals face B of plasma membrane (pm_B), bilayer membrane diaphragm ($d_B{}^{pm}$), concave particle-poor network (ut_B), and convex particle-rich network (lt_A). ut_B is continuous with pm_B; lt_A is not and points of contiguity with plasma membrane (arrows) illustrate tunnel-like nature of network (see Discussion II, 3). This is also illustrated at points of contiguity of convex (lt_A) and concave (ut_B) networks (opposed arrowheads). × 140,000.

brane; (*b*) the inner dense line of the bilayer membrane diaphragm appears continuous with the inner dense line of the peripheral vesicle membrane; and (*c*) the outer dense line of the peripheral vesicle membrane appears continuous with the inner dense line of the plasmalemma. Frequently, the regions adjoining the bilayer membrane diaphragm were electron dense (Figs. 12

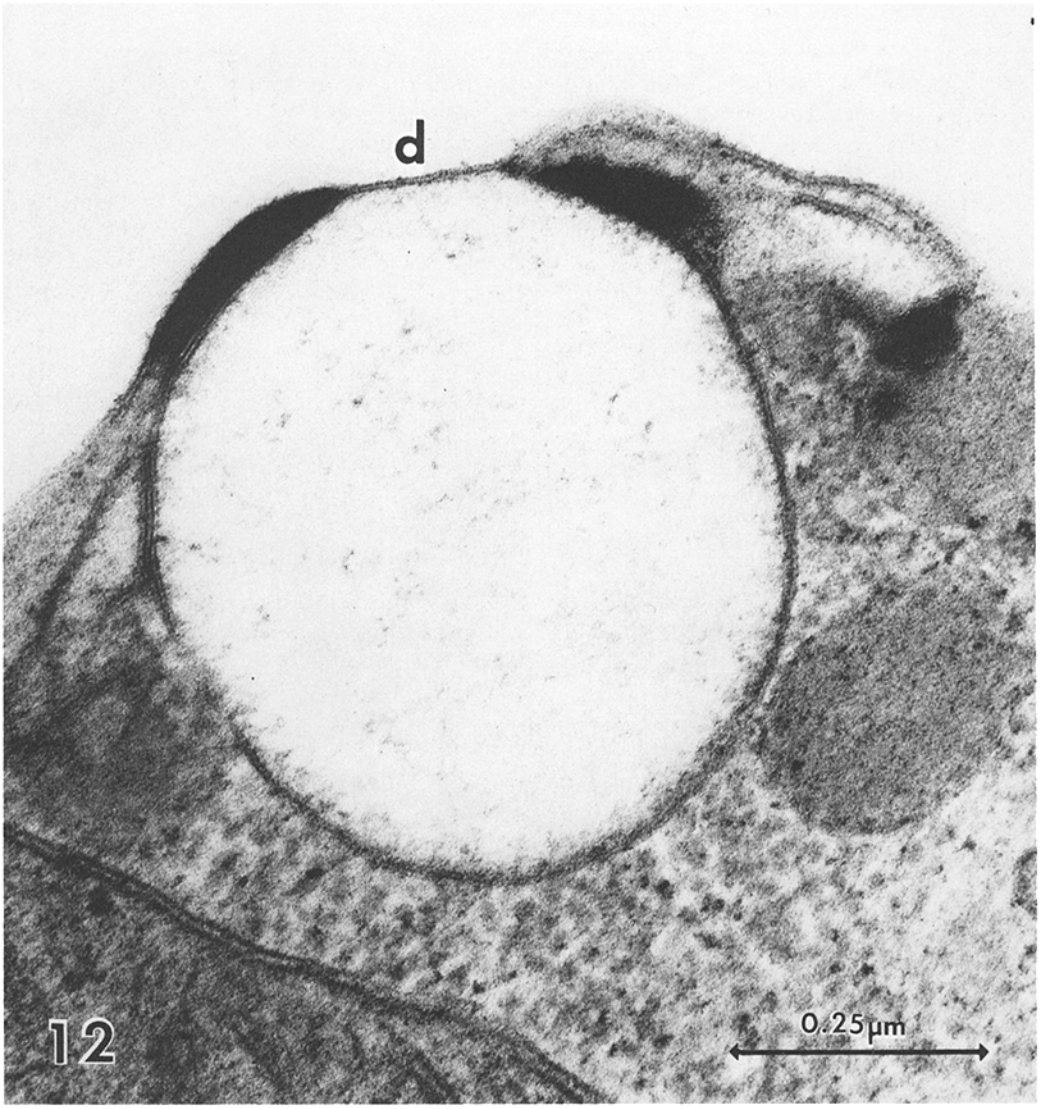

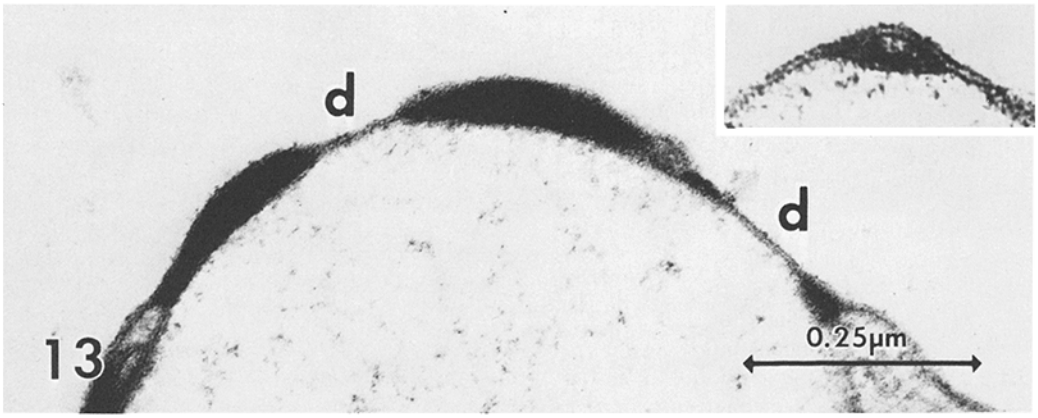

FIGURE 12 Thin section of peripheral vesicle fused with plasmalemma. Vesicle lumen is separated from external medium by a bilayer membrane diaphragm (*d*, seen here as a trilaminar profile). Electron-dense regions are seen close to the diaphragm. × 140,000.

FIGURE 13 Area of fusion of peripheral vesicle with plasmalemma. Bilayer membrane diaphragms (*d*) are interrupted by tunnels with an electron-dense lumen. These tunnels seem delimited on both sides by membranes (see inset). × 125,000; inset × 240,000.

and 14). Regions with similar electron density could also be seen interrupting the bilayer membrane diaphragm (Fig. 13). These regions appeared delimited on both sides by a membrane (Fig. 13, inset), although this was difficult to establish because the high electron density of the lumina generally obscured the thin-section profile of the delimiting membrane. Occasionally, trilaminar membrane profiles were also observed between two adjacent, fused peripheral vesicles (Fig. 15). Again, electron-dense regions were observed adjoining the areas of fusion although the diaphragm was not interrupted by membrane-delimited dense areas.

DISCUSSION

I Interpretation of Results

(*a*) Freeze-fracture

The interpretation of our freeze-fracture observations is diagrammatically presented in Fig. 16. We think that all our observations can be accounted for if the complex of fracture faces is viewed to represent stages intermediary between the initial event of fusion and the release of the peripheral vesicle contents to the extracellular space. The smooth fracture faces ($d_B{}^{pm}$ and $d_B{}^{v}$) are interpreted as representing particle-free diaphragms with bilayer membrane organization. The diaphragms coexist and delimit a polymorphic network of tunnels. Tunnels and diaphragms are continuous with both the surrounding plasma membrane and the vesicle membrane.

To assess our interpretation, we have used a schematic membrane system to predict the types of fracture faces that could coexist on any given fracture alternative as shown in Fig. 16*b*. The solid line depicts the course of the fracture face, generally following the plasma membrane rather than the peripheral vesicle membrane (dotted line). The latter alternative, although possible is much less probable due to its unfavorable geometry (fracture tends to follow the easiest course); as a consequence, simultaneous views of pm_B and v_A (Fig. 9) or of pm_A and v_B (Fig. 8) are rare. The membrane tunnels have been arbitrarily divided into "upper tunnel" (*ut*) and "lower tunnel" (*lt*) denoting, respectively, regions of the tunnel convex to the exterior or to the interior of the cell.

The general fracture scheme predicts two sets of coexisting fracture faces (Fig. 16*b*, I and II): [pm_A-$d_B{}^{v}$-ut_A-lt_B-(v_B)]; and [pm_B-$d_B{}^{pm}$-ut_B-lt_A-(v_A)]. We assume that regions of the upper tunnel represent membrane originally belonging to the plasma membrane; and the lower tunnel membrane originally part of the peripheral vesicle. Consequently, according to our interpretations: (*a*) ut_A should be particle-rich and convex; (*b*) ut_B, particle-poor and concave; (*c*) lt_B, particle-poor and concave; and (*d*) lt_A, particle-rich and convex. This is schematically presented in Fig. 16*b*. Using this scheme, we analyzed all the profiles of fusion in order to ascertain whether or not our interpretation was consistent with the experimental results. In no case did we find a fracture face which was not consistent with the predictions of our interpretation. This is illustrated in the labels and legends of Figs. 2–11.

(*b*) Thin Section

Our thin-section observations are consistent with the interpretation illustrated in Fig. 16 and confirm the presence of a bilayer membrane diaphragm seen as a trilaminar profile which appears common to both the plasmalemma and the peripheral vesicle (Figs. 12–14). As described, the plasma membrane seems to join the vesicle membrane in a "Y" profile (Fig. 14, opposed arrows) in which the inner dense line of the plasmalemma is continuous with the outer dense line of the vesicle membrane and forms a "hinge," whereas the outer dense line of the plasmalemma joins the inner dense line of the peripheral vesicle membrane to form the trilaminar profile of the diaphragm.

II Membrane Fusion: A Hypothesis

(*a*) Introduction

Membrane fusion, in order to occur, requires the fulfillment of two crucial events (29): (*a*) approximation and contact, and (*b*) induction of fusion. It is clear that our morphological observations cannot directly illustrate the second, very important step. Consequently, we will limit our hypothesis to the sequence of events that follow the induction of fusion. Our hypothesis will have to: (*a*) explain the existence of a particle-free or particle poor bilayer membrane diaphragm; (*b*) account for the formation of a polymorphic network of tunnels; (*c*) propose continuity between the bilayer membrane diaphragm and the membranes which form the tunnels with the plasma membrane and the peripheral vesicle membrane; (*d*) explain the occasional presence of large,

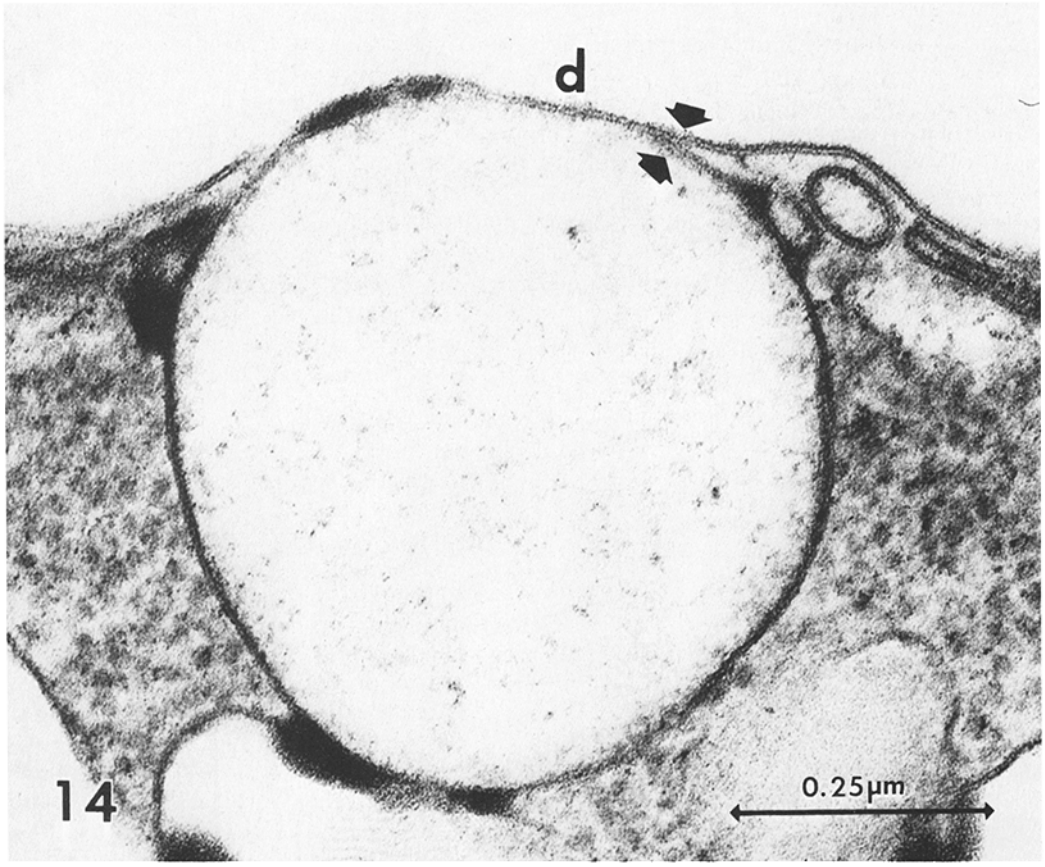

FIGURE 14 Peripheral vesicle fused with plasmalemma. Trilaminar profile of the bilayer membrane diaphragm is clear. Double arrows indicate region where the outer dense line of diaphragm appears continuous with the outer dense line of peripheral vesicle membrane and the inner dense line of diaphragm appears continuous with the inner dense line of the peripheral vesicle membrane. Continuity between the inner dense line of the plasma membrane and the outer dense line of the peripheral vesicle membrane is suggested. × 140,000.

FIGURE 15 Two mutually fused peripheral vesicles share a common membrane. × 90,000.

rounded particles on the fracture faces of the bilayer membrane diaphragm; (*e*) provide reasons which may account for the release of the vesicular contents to the extracellular space; and (*f*) be consistent with the action of known inducers of membrane fusion.

(*b*) Steps during Fusion

We propose the following hypothesis.

1 FUSION OF CONTACTING MEMBRANE MONOLAYERS: At present, we cannot hypothesize the molecular mechanisms responsible for the induction of fusion. They are known to vary because different agents can induce membrane fusion (17, 29, 30), although the possibility exists of a common subterminal mechanism (e.g., induced by an increase in the cytoplasmic free Ca^{++} concentration). It is clear, however, that fusion represents a transition between two noncontinuous states, involving profound, probably sudden reorganization of membrane components. In Thom's sense (38), it probably represents a localized catastrophe.

We propose that the initial fusion event results in structural continuity of the apposed monolayers of the fusing membranes (in our case, the inner half of the plasmalemma and the outer half of the peripheral vesicle) along the perimeter of the site of fusion, i.e., the formation of a single membrane monolayer (Fig. 17 A). Due to the geometry of the system, this originates a ring-like hinge around the site of fusion which we consider a toroid hemimicelle (Fig. 17, dotted wedges). Depending on the extension of the site of fusion, membrane components from the apposing monolayers may remain trapped within the perimeter of fusion which may (or may not) reorganize into an inverted membrane micelle sequestered within a hydrophobic milieu (Fig. 17 A, dotted circle). In principle, the molecular components of either the toroid hemi-micelle or the inverted membrane micelle may include not only membrane lipids but also membrane proteins.

2 FORMATION OF BILAYER MEMBRANE DIAPHRAGMS: Fusion of the apposing, proximal (relative to the plane of apposition) membrane monolayers causes approximation of lipid components from the nonapposed, distal membrane monolayers (Fig. 17 A and B). In a secretory process, this will involve the outer half of the plasma membrane and the inner (exoplasmic) half of the secretory vesicle membrane. Approximation of the distal membrane monolayers is likely due to the presence of excess membrane components in these monolayers relative to the proximal monolayers, as components of the latter will have been used in the formation of the toroid hemimicelle and, if this be the case, the inverted membrane micelle. Thermodynamically, this interaction is a favored event because it will involve the establishment of van der Waals contacts between apolar lipid chains of the distal membrane monolayers. This apposition will result in the formation of a small bilayer membrane diaphragm (Fig. 17 B).

Radial expansion of the bilayer membrane diaphragm will be possible through centrifugal expansion of the perimeter of the toroid hemi-micelle through insertion of additional components from the proximal membrane monolayers. Expansion of the bilayer membrane diaphragm will depend on the position of equilibrium between the forces stabilizing the bilayer membrane diaphragm as it is formed and those which arise during compression of membrane components in the proximal membrane monolayers caused by the centrifugal expansion of the toroid hemi-micelle. The extent of the expansion of the bilayer membrane diaphragm will also depend on the geometry of the system, mainly the radius of curvature of the fusing membranes and whether or not one membrane is, topogically, internal to the other.

The mechanism of bilayer membrane diaphragm formation outlined above accounts for the absence or rarity of particles on the fracture face of the diaphragm. The membrane particles probably represent protein-containing structures intercalated across membrane domains with bilayer organization (8, 12, 16, 19, 26–28). Consequently, although lipids and peripheral membrane proteins (and also putative integral membrane proteins associated only with one membrane half) can, in principle, flow from the outer half of the plasma membrane or from the inner half of the peripheral vesicle membrane into the diaphragm, this is not possible for structures intercalated across both halves of the membrane (Fig. 17).[3]

[3] Passage of such a structure (Fig. 17) from the membrane into the diaphragm bilayer membrane is thermodynamically unfavorable because it will involve passage of polar portions of the intercalation across the apolar matrix of the inner membrane half and insertion of those hydrophilic regions across the inner half of the diaphragm bilayer membrane in order to reexpose them to the aqueous environment of the vesicle lumen. Passage into the diaphragm would be possible in cases where the protein spans only one half of the membrane or in the case of hypothetical components, totally sequestered

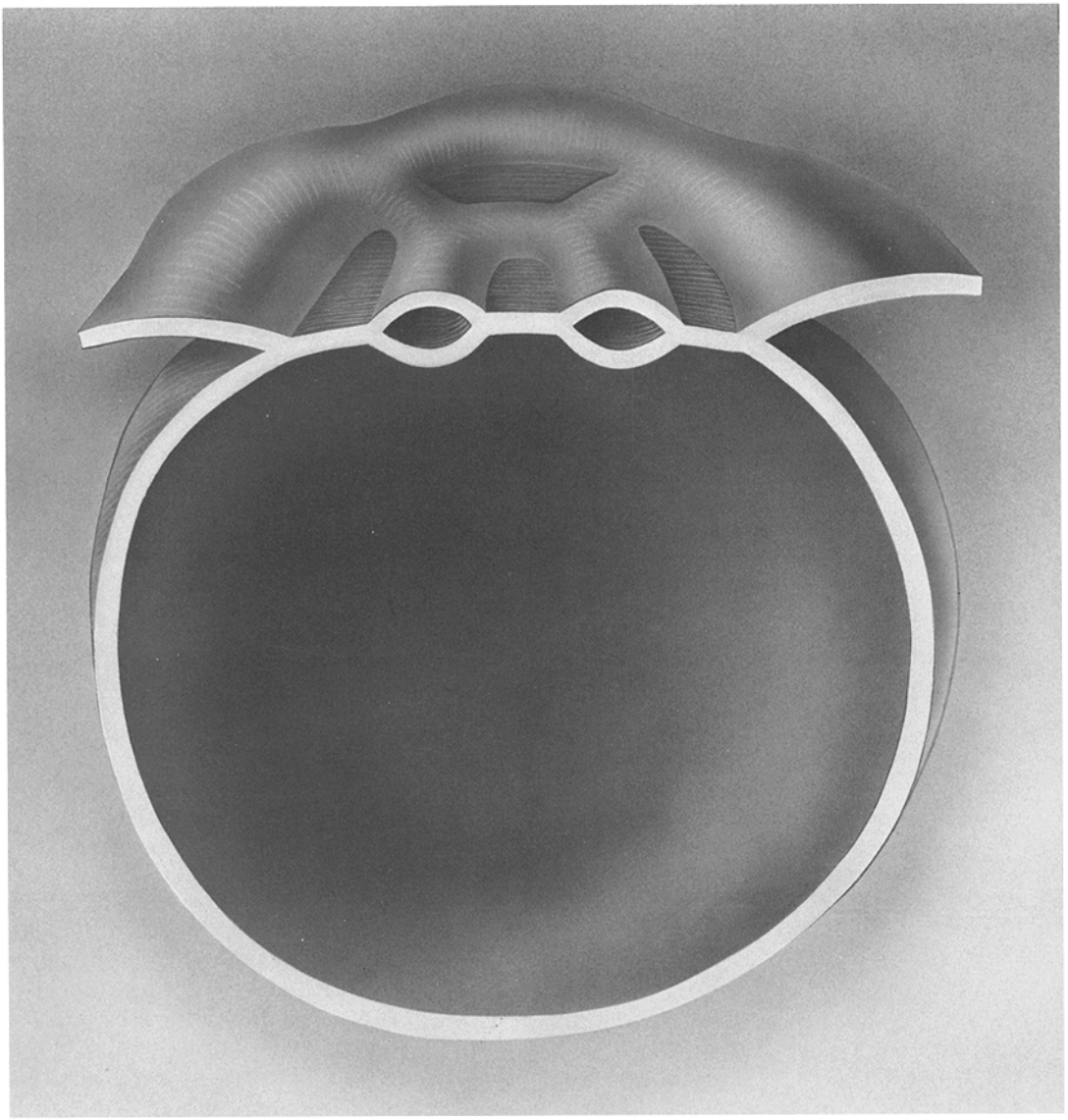

FIGURE 16 *a* Proposed three-dimensional representation of *P. palmivora* plasmalemma and peripheral vesicle during fusion.

3 FORMATION OF A NETWORK OF TUNNELS CONTINUOUS WITH THE PLASMALEMMA AND THE VESICLE MEMBRANE: If, as in *P. palmivora* zoospores, the area of close approximation and contact is sufficiently large, several fusion events may occur along the contact zone. Bilayer membrane diaphragm formation and expansion at these points will result in the formation of a polymorphic system of membrane-delimited tunnels through restriction of the area of unfused plasma membrane and vesicular membrane. The lumen of the tunnels will be continuous with the cytoplasm but separate from the extracellular space or the vesicular lumen (Fig. 16*a*). It is clear that the tunnels will not be formed if the contact

within the hydrophobic matrix of the membrane (Fig. 17). Inverted membrane micelles produced during fusion could, in principle, cross beyond the toroid hemi-micelle into the plasma membrane or the vesicle membrane because they are sequestered within the apolar matrix of the bilayer membrane diaphragm (Fig. 17). Intercalated particles may, due to their incapacity to penetrate into the diaphragm, accumulate at the edge of the toroid hemi-micelle. However, due to planar diffusion gradients, these particles may also be removed from the edge.

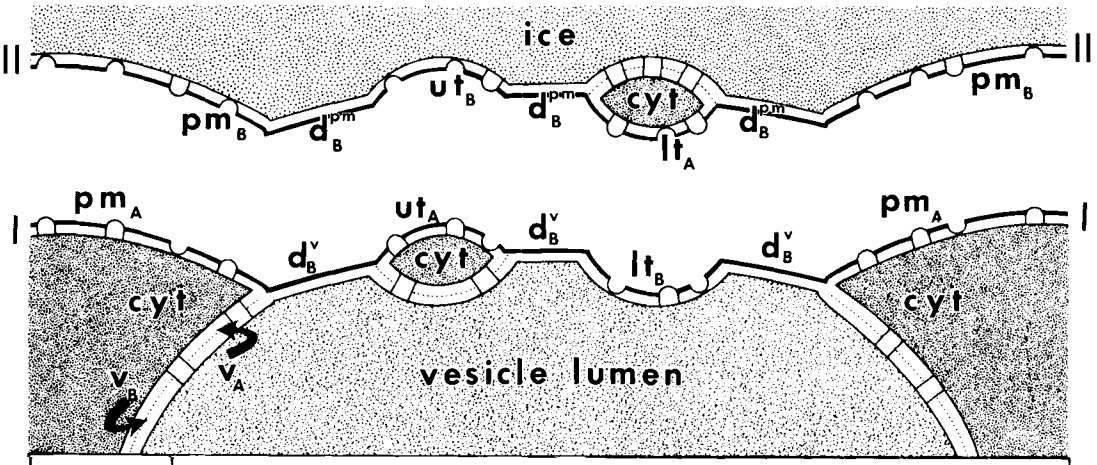

		pm_A	v_B	d_B^v	ut_A	lt_B
I	PARTICLES	++	+	0	++	+
	SHAPE	CONVEX	CONVEX	SLIGHTLY CONVEX OR FLAT	CONVEX	CONCAVE
		pm_B	v_A	d_B^{pm}	ut_B	lt_A
II	PARTICLES	+	++	0	+	++
	SHAPE	CONCAVE	CONCAVE	SLIGHTLY CONCAVE OR FLAT	CONCAVE	CONVEX

FIGURE 16 *b* Schematic representation of faces produced by freeze-fracture. Freeze-fracture produces two sets of fracture faces; I and II. Fracture of peripheral vesicle membrane, less frequent, exposes v_A (see Fig. 9) and v_B (see Fig. 8). *pm*, plasma membrane; *d*, particle-free bilayer membrane diaphragm; *ut*, upper region of membrane tunnel; *lt*, lower region of membrane tunnel; *v*, peripheral vesicle membrane; ++, particle-rich; +, particle-poor; 0, no particles or isolated large particles (micelles); *cyt*, cytoplasm.

area for fusion is small, leading to a single event of fusion and, consequently, a single bilayer membrane diaphragm.

4 RELEASE OF VESICULAR CONTENTS: The events described result in the formation of a new membrane with new characteristics—a bilayer membrane diaphragm—which separates the lumen of the vesicle from the cell exterior. As discussed above, the bilayer membrane diaphragm originates at the outer half, from a selection of components from the outer half of the plasma membrane and, at the inner half, from a selection of components from the inner (exoplasmic) half of the peripheral vesicle membrane. Therefore, the bilayer membrane diaphragm can be considered as a modified hybrid of two half membranes with separate origin. We face also an important modification of the topological relationships of the spaces delimited by the membrane system, from two concentric, closed surfaces to a hybrid system in which the environment surrounding the vesicle is, simultaneously, cytoplasm and outside medium (Figs. 12 and 14). Either of these changes (and, more so, their joint presence) is likely to alter the balance (ionic, osmotic) of the vesicle relative to its environment. This is a metastable situation which may lead, directly or indirectly, to rupture of the diaphragm, release of the secretory products, and incorporation of the peripheral vesicle membrane into the plasmalemma. Although the bilayer membrane diaphragm seems to be under tension, its frequent observation in our system makes it likely that, in *P. palmivora*, it persists for a relatively long period (i.e., over at least a few seconds) before it ruptures.

III Congruence of Hypothesis with Experimental Observations

An essential feature of our hypothesis of membrane fusion is the formation of a bilayer membrane diaphragm. Our experiments demonstrate that a diaphragm with bilayer membrane organiza-

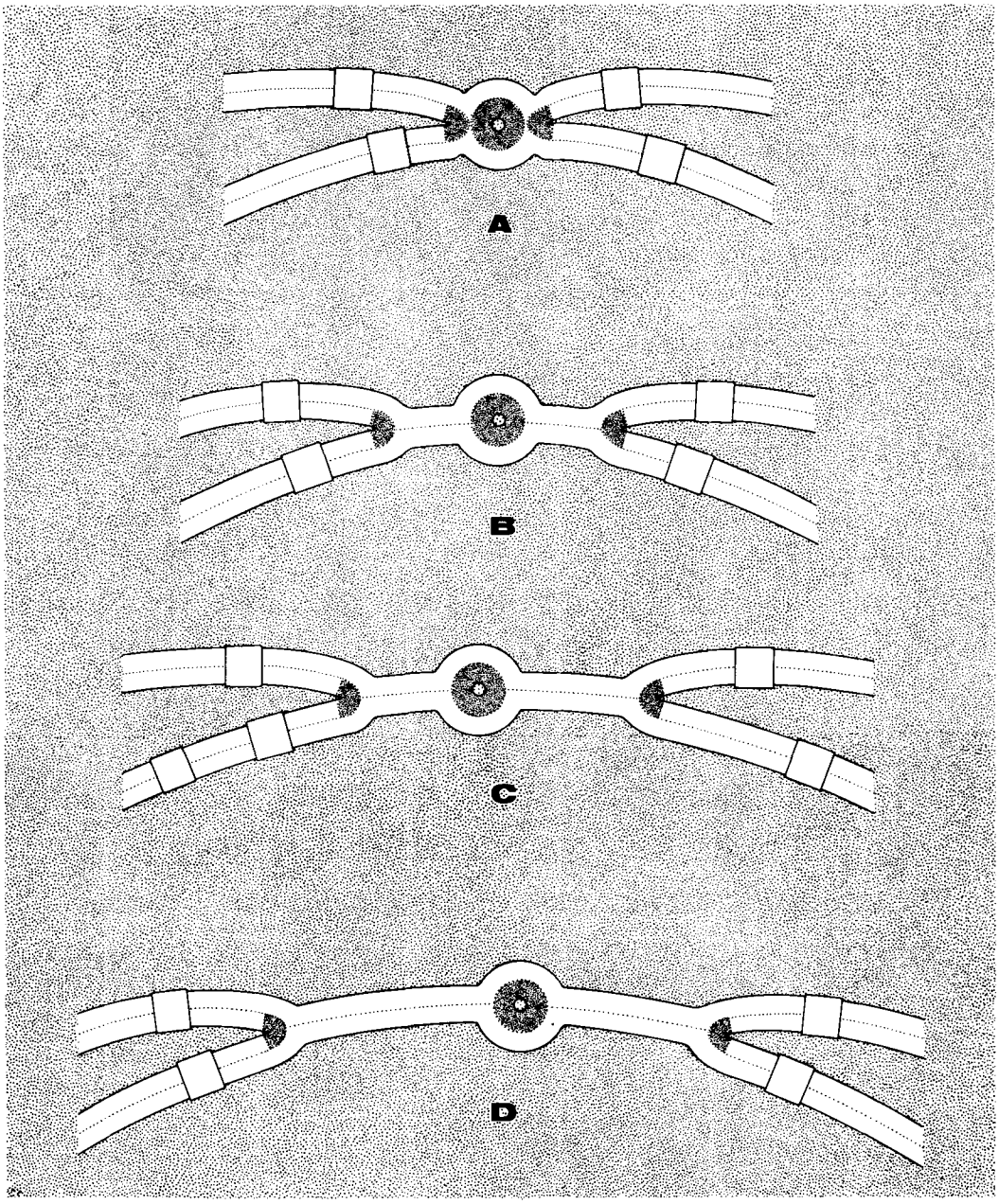

FIGURE 17 Diagram represents steps during membrane fusion leading to formation of bilayer membrane diaphragm. Dotted line follows hydrophobic juncture which is split during freeze-fracture. Heavily dotted areas represent postulated inverted membrane micelle (circular) and toroid hemi-micelle (wedges). Lipids, as well as peripheral membrane proteins (and also, putative integral membrane proteins associated with one membrane half) may flow from either the outer half of the plasma membrane or the inner (exoplasmic) half of the vesicle membrane into the bilayer membrane diaphragm. Membrane particles (squares) are thought to represent protein-containing intercalations, and cannot penetrate into the bilayer membrane diaphragm.

tion is formed during fusion of peripheral vesicles with the plasma membrane of *P. palmivora* zoospores. As shown, freeze-fracture of fusing membranes demonstrates a smooth face almost devoid of particles (the bilayer membrane diaphragm). This structure is clearly distinguishable from that which is produced by ice (i.e., should an aqueous continuity exist between the lumen of the fused membrane and the extracellular space). Thin sections also demonstrate the presence of a bilayer membrane diaphragm (seen as a trilaminar profile) which appears continuous with the outer half of the plasma membrane and the inner (exoplasmic) half of the peripheral vesicle membrane.

Occasionally, examination of the fracture faces of bilayer membrane diaphragms reveals the presence of large, rounded particles (Fig. 5; Fig. 10, asterisk) and depressions (Fig. 8, arrowheads). Fig. 4 shows that the rounded depressions (solid arrowheads) coexist with very small diaphragms (hollow arrowheads). These probably represent an initial stage of fusion. Although we realize that our evidence is circumstantial, it is possible that the isolated, rounded particles and depressions observed on the fracture faces of bilayer membrane diaphragms represent inverted membrane micelles which may be formed during the initial stages of the fusion process (Fig. 17). As discussed, these structures are thought to be totally sequestered within the hydrophobic environment of the bilayer membrane diaphragm. The depressions left by these structures on the apposed fracture face are very clear (Fig. 8, arrowheads) in contrast to those left by plasma membrane particles which are generally difficult to resolve.

Examination of the results of previous ultrastructural investigations of membrane fusion also reveals the presence of bilayer membrane diaphragms as intermediary stages during membrane fusion. In a study of the fusion of vesicles with the distal membrane of endothelial blood capillaries, Palade and Bruns (24) first reported the presence of bilayer membrane diaphragms and proposed that similar structures might be formed during formation of endothelial fenestrae. This seems to be illustrated in a freeze-fracture study which shows smooth fenestrae with a fracture plane which is continuous with that of the plasmalemma (11).[4] Most of these fenestrae contain a knob (diameter ~11 nm) that is easily distinguished from the membrane particles by its size, irregular shape, and smooth contour. Significantly, the position of the knob on the diaphragm is variable: frequently central, in other instances close to the edge or even straddling (as if migrating) across the edge of the diaphragm (reference 11, Fig. 1). The diaphragm fracture face is observed to be continuous with the fracture faces of proximal and distal endothelial plasma membranes.

The formation of bilayer membrane diaphragms during fusion can be found in micrographs included in the freeze-fracture study of membrane fusion during mucocyst secretion (33, 34).[5] Here, a rosette of particles (diameter ~60 nm) appears on the region of the plasma membrane which is fusing with the secretory vesicle. The area delimited by the rosette is smooth, with the exception of a central particle. Satir and co-workers report that continuation of the process of fusion results in circular expansion of the area delimited by the rosette and disappearance of the central particle.[6] The circular area is smooth and reaches a maximum diameter of about 210 nm, representing an expansion in area of about twelve times (reference 33, Fig. 19). We believe that this particle-free area represents a bilayer membrane diaphragm because it is smooth and because it is not etchable

[4] Freeze-fracture of capillary fenestrae generally reveals a granular and irregular appearance (32) due to the absence of a cleavage plane in the single-layered fenestrae. Note the close similarity of capillary fenestrae and nuclear pores in both thin section and freeze-fracture (9, 10, 20, 21, 31).

[5] Small, particle-free diaphragms may also be observed in other freeze-fracture studies (reference 22, Fig. 1 *c,d;* reference 36, Fig. 1 *a,b*). However, these are small and could be interpreted as vitreous ice.

[6] It is possible that the particle seen at the center of the rosette represents the inverted membrane micelle that may be at the origin of the actual fusion event. Significantly, it is reported that the central particle of the rosette adheres with fracture faces A and B with similar frequency (0.5 and 0.4, respectively (34). This contrasts with the particles of the rosette which show, as do other membrane particles, a much higher frequency on fracture face A. Equal frequency of association could be expected if the central particle represented a membrane micelle sequestered within the hydrophobic interior of the diaphragm because the micelle should not have, in principle, preferential association with any membrane half. It is also interesting to note that while the diaphragm remains free of particles, particles can be seen accumulated at the edge of the expanded diaphragm. Disappearance of the central particle during expansion of the diaphragm is also consistent with our hypothesis as discussed in footnote 3.

(i.e., sublimable). Satir and co-workers view the region comprised within the rim of fusion as composed of two separate membrane halves. According to this interpretation, the nonetchable face produced at the opening represents contact with the hydrophobic side of a membrane monolayer (reference 3, Fig. 1*c*). This interpretation seems unlikely because the existence of a separate membrane half immersed on both sides in an aqueous environment is thermodynamically unfavorable.

Recently, bilayer membrane diaphragms were also reported during fusion of mucous droplets with the luminal plasma membrane in acinar cells (37), and lipid bilayer diaphragms during the formation of a stable doublet by apposing phospholipid spherical membranes (7). It has also been proposed that membrane apposition of particle-free areas may be a condition necessary to fusion (1). In such areas the membrane lipids would be perturbed, possibly assuming a semimicellar configuration which could allow intermembrane hydrophobic interactions (7). Our hypothesis is compatible with these concepts although it does not, in principle, rule out the participation of nonintercalated membrane proteins from initial fusion events.

We believe that, in membrane systems, analysis of topological relationships and of their thermodynamic consequences precedes and helps to define domains where structural solutions are to be found. In this paper we have reported the freeze-fracture and thin-section morphology of the plasmalemma and peripheral vesicles during the initial stages of encystment of *P. palmivora* zoospores and attempted to define a sequence of events during membrane fusion with particular emphasis on changes in topological relationships. We believe that this sequence is compatible with our experimental results and with those which we could analyze from the literature.

At present we do not know the mechanisms which lead to the initiation of fusion or to the rupture of the bilayer membrane diaphragm and release of secretory product.

We wish to thank Drs. S. Bartnicki-Garcia and P. Gullino for helpful discussions, Dr. D. E. Hemmes for the generous supply of plastic embedded zoospores, Dr. H. H. R. Friederici for original micrographs of freeze-fractured capillary endothelium, and Miss Patricia Torreyson, Mr. Bela Berghoffer and Mr. Clifford Parkison for technical assistance.

The work was supported in part by U.S. Public Health Grant CA-15114 from the National Cancer Institute (to Pedro Pinto da Silva) and a fellowship from the Organization of American States (to Maria Luiza Nogueira).

Received for publication 23 August 1976, and in revised form 29 November 1976.

REFERENCES

1. Ahkong, O. F., D. Fisher, W. Tampion, and J. A. Lucy. 1975. Mechanisms of cell fusion. *Nature (Lond.).* **253:**194–195.
2. Aragaki, M., and R. B. Hine. 1963. Effect of radiation on sporangial production of *Phytophthora parasitica* on artificial media and detached papaya fruit. *Phytopathology.* **53:**854–856.
3. Bartnicki-Garcia, S. 1973. Cell wall genesis in a natural protoplast: the zoospore of *Phytophthora palmivora*. *In* Yeast, Mould and Plant Protoplast. J. R. Villaneuva, I. Garcia-Acha, S. Gascon, and F. Uruburu, editors. Academic Press, London. 77–91.
4. Bartnicki-Garcia, S., and D. E. Hemmes. 1976. Some aspects of the form and function of oomycete spores. *In* B. J. Weber, and H. M. Hess, editors. The Fungal Spore: Form and Function. John Wiley & Sons, Inc., New York. 593–641.
5. Branton, D. 1966. Fracture faces of frozen membranes. *Proc. Natl. Acad. Sci. U.S.A.* **55:**1048–1052.
6. Branton, D., S. Bullivant, N. Gilula, M. Karnovsky, H. Moor, K. Mühlethaler, D. Northcote, L. Packer, B. Satir, P. Satir, V. Speth, L. Staehelin, R. Steere, and R. Weinstein. 1975. Freeze-etching nomenclature. *Science (Wash. D.C.).* **190:**54–56.
7. Breisblatt, W., and S. Ohki. 1975. Fusion in phospholipid spherical membranes. I. Effect of temperature and lysolecithin. *J. Membr. Biol.* **23:**385–401.
8. Deamer, D. W. 1973. Isolation and characterization of a lysolecithin-adenosine triphosphatase complex from lobster muscle microsomes. *J. Biol. Chem.* **248:**5477–5485.
9. Franke, W. W. 1974. Nuclear envelopes. Structure and biochemistry of the nuclear envelope. *Philos. Trans. R. Soc. Lond. B. Biol. Sci.* **268:**67–93.
10. Friederici, H. H. R. 1968. The tridimensional ultrastructure of fenestrated capillaries. *J. Ultrastruct. Res.* **23:**444–456.
11. Friederici, H. H. R. 1969. On the diaphragm across fenestrae of capillary endothelium. *J. Ultrastruct. Res.* **27:**373–375.
12. Grant, W. M., and H. M. McConnell. 1974. Glycophorin in lipid bilayers. *Proc. Natl. Acad. Sci. U.S.A.* **71:**4653–4657.
13. Grove, S. N. 1971. Protoplasmic correlates of hyphal tip initiation and development in fungi. Ph.D. Dissertation. Purdue University, West Lafayette, Ind.
14. Hemmes, D. E., and H. R. Hohl. 1971. Ultra-

structural aspects of encystation and cyst germination in *Phytophthora parasitica*. *J. Cell. Sci.* **9**:175–191.

15. Ho, H. H., K. Zachariah, and C. J. Hickman. 1968. Ultrastructure of zoospores of *Phytophthora megasperma* var. *sojae*. *Can. J. Bot.* **46**:37–41.
16. Hong, K., and W. L. Hubbell. 1972. Preparation and properties of phospholipid bilayers containing rhodopsin. *Proc. Natl. Acad. Sci. U.S.A.* **69**:2617–2621.
17. Lucy, J. A. 1970. The fusion of biological membranes. *Nature (Lond.)*. **227**:815–817.
18. Marchesi, V., and H. Furthmayer. 1976. The red cell membrane. *Ann. Rev. Biochem.* **45**:667–698.
19. Marchesi, V. T., T. W. Tillack, R. L. Jackson, J. P. Segrest, and R. D. Scott. 1972. Chemical characterization and surface orientation of the major glycoprotein of the human erythrocyte membrane. *Proc. Natl. Acad. Sci. U.S.A.* **69**:1445–1499.
20. Maul, G. 1971. Structure and formation of pores in fenestrated capillaries. *J. Ultrastruct. Res.* **36**:768–782.
21. Maul, G. D., J. W. Price, and M. W. Lieberman. 1971. Formation and distribution of nuclear pore complexes in interphase. *J. Cell Biol.* **51**:405–418.
22. Orci, L., M. Amherdt, F. Malaisse-Lagae, C. Rouiller, and A. E. Renold. 1973. Insulin release by emiocytosis: Demonstration with freeze-etching technique. *Science (Wash. D.C.)*. **179**:82–83.
23. Palade, G. 1975. Intracellular aspects of the process of protein synthesis. *Science (Wash. D.C.)*. **189**:347–358.
24. Palade, G., and R. R. Bruns. 1968. Structural modulations of plasmalemmal vesicles. *J. Cell. Biol.* **37**:633–649.
25. Pinto da Silva, P., and D. Branton. 1970. Membrane splitting in freeze-etching. Covalently labelled ferritin as a membrane marker. *J. Cell Biol.* **45**:598–605.
26. Pinto da Silva, P., S. D. Douglas, and D. Branton. 1971. Localization of A antigen sites on human erythrocyte ghosts. *Nature (Lond.)*. **232**:194–196.
27. Pinto da Silva, P., P. Moss, and H. H. Fudenberg. 1973. Anionic sites on the membrane intercalated particles of human erythrocyte ghost membranes. Freeze-etch localization. *Exp. Cell Res.* **81**:127–138.
28. Pinto da Silva, P., and G. Nicolson. 1974. Freeze-etch localization of Concanavalin A receptors to the membrane intercalated particles in human erythrocyte membranes. *Biochim. Biophys. Acta.* **363**:311–319.
29. Poste, G., and A. C. Allison. 1971. Membrane fusion reaction: a theory. *J. Theor. Biol.* **32**:165–184.
30. Poste, G., and A. C. Allison. 1973. Membrane fusion. *Biochim. Biophys. Acta.* **300**:421–465.
31. Rhodin, J. A. G. 1962. The diaphragm of capillary endothelial fenestrations. *J. Ultrastruct. Res.* **6**:171–185.
32. Ryan, U. S., J. W. Ryan, D. S. Smith, and H. Winkler. 1975. Fenestrated endothelium of the adrenal gland: freeze-fracture studies. *Tissue Cell.* **7**:181–190.
33. Satir, B., C. Schooley, and P. Satir. 1972. Membrane reorganization during secretion in *Tetrahymena*. *Nature (Lond.)*. **235**:53–54.
34. Satir, B., C. Schooley, and P. Satir. 1973. Membrane fusion in a model system. Mucocyst secretion in *Tetrahymena*. *J. Cell Biol.* **56**:153–176.
35. Sing, V. O., and S. Bartnicki-Garcia. 1975. Adhesion of zoospores of *Phytophthora palmivora*. Detection and ultrastructural visualization of Concanavalin A receptor sites appearing during encystment. *J. Cell Sci.* **19**:11–20.
36. Smith, U., D. S. Smith, H. Winkler, and J. W. Ryan. 1973. Exocytosis in the adrenal medulla demonstrated by freeze-etching. *Science (Wash. D.C.)*. **179**:79–82.
37. Tandler, B., and J. J. Poulsen. 1976. Fusion of the envelope of mucous droplets with the luminal plasma membrane in acinar cells of the cat submandibular gland. *J. Cell Biol.* **68**:775–781.
38. Thom, R. 1972. Stabilité Structurelle et Morphogénèse. Essai d'Une Théorie Générale des Modèles. W. A. Benjamin, Inc., Reading, Mass.
39. Tokunaga, J., and S. Bartnicki-Garcia. 1971. Cyst wall formation and endogenous carbohydrate utilization during synchronous encystment of *Phytophthora palmivora* zoospores. *Arch. Mikrobiol.* **79**:283–292.